JOURNAL OF GEOPHYSICAL RESEARCH, VOL. 103, NO. B7, PAGES 15,051–15,068, JULY 10, 1998

Anomalous surface waves from Lop Nor nuclear explosions: Observations and numerical modeling

Helle A. Pedersen
Laboratoire de Géophysique Interne et Tectonophysique, Université Joseph Fourier Grenoble, France

Jean-Philippe Avouac
Laboratoire de Détection et de Géophysique, Bruyères-le-Châtel, France

Michel Campillo [1]
Laboratoire de Géophysique Interne et Tectonophysique, Université Joseph Fourier Grenoble, France

Abstract. Surface waves from the Chinese test site of Lop Nor are analyzed using long-period and broadband stations located at regional and teleseismic distances and at different azimuths. For most azimuths, strong Love waves between 0.02 and 0.045 Hz are observed with an amplitude of up to 10 times that of the Rayleigh waves. In addition, an anomalous early Rayleigh wave train is observed at some stations in western Europe. Due to a particularly favorable station and source configuration, it is possible to isolate the areas where the anomalies are created. The high-amplitude Love waves must be attributed to either source effects or path effects immediately north of Lop Nor. The early wave train is shown to be due to a partial energy conversion between Love and Rayleigh waves, probably at the Tornquist Zone. To estimate the possible contribution from surface wave conversions to the observed anomalies, numerical simulations are carried out with the indirect boundary element method. The simulations show that a relatively small variation of crustal thickness can induce Rayleigh to Love wave conversions between 0.02 and 0.1 Hz frequency. The calculated amplitudes of the Love waves are significant (up to 35% of the amplitude of the incoming Rayleigh waves), but they are too small to fit the observed amplitude anomaly. The observed converted waves and the numerical results nevertheless indicate that surface wave conversions can be significant across strong lateral crustal heterogeneities. In particular, the conversions due to changes in crustal thickness are located in the period interval which is routinely used for estimation of *Ms*.

1. Introduction

Recent developments of permanent and temporary broadband arrays have drawn attention to the use of surface waves for investigating the seismic velocities in the deep crust and upper mantle and their lateral variation. Lateral inhomogeneities may result in off great circle propagation paths and strong diffractions, giving rise to reflected and refracted surface waves as well as wave conversions between different types of waves and between different surface wave modes. The existence of at least one type of diffracted surface waves is well established. These are multiple arrivals, typically of 10-40s period, within the late part of the fundamental mode surface waves [e.g., *Capon,* 1970; *Levshin and Ritzwoller,* 1995]. Array analysis of these waves shows that they can significantly deviate from the great circle path [e.g., *Capon,* 1970; *Pavlis and Mahdi,* 1996]. Another diffraction effect is the strong amplitude variations of fundamental mode Rayleigh waves that are observed for some specific paths [*McGarr,* 1969] along which wave refraction occurs. An example of modeling of such effects is given by *Tanimoto* [1990].

The diffraction effects have direct consequences for monitoring purposes, as they can introduce significant amplitude anomalies and consequently influence esti-

[1] Also at Institut Universitaire de France

Paper number 98JB00027.
0148-0227/98/98JB-00027$09.00

mations of the seismic moment tensor. Unfortunately, these effects are not easily detectable, especially at intermediate periods (20-40 s) as the Love and Rayleigh waves overlap in time. For example, a low-amplitude, 30 s Love to Rayleigh converted wave would typically arrive within the longer-period part of the Rayleigh wave train. Some path effects will therefore routinely be attributed to the seismic source and in the case of nuclear explosions have consequences in the estimation of yield and tectonic release.

Tectonic release is a term which covers different physical phenomena related to wave radiation in prestressed media, for example, rock failure [e.g., *Press and Archambeau,* 1962; *Archambeau and Sammis,* 1970] or stress release on neighboring faults [e.g., *Aki and Tsai,* 1972]. Even though the existence of tectonic release is clearly established for a large number of explosions, it is nevertheless difficult to clearly distinguish between different mechanisms of tectonic release because none of them explain all observations in a satisfactory way (for a review, see *Massé* [1981]). Quantitative modeling of tectonic release is also difficult because nonlinear effects must be taken into account [e.g., *Harkrider et al.,* 1994].

The aim of this paper is to show that path effects can significantly influence surface waves as recorded at teleseismic distances from the Chinese nuclear test site of Lop Nor. Such path effects must be taken into account when source anomalies of Lop Nor explosions are studied.

We systematically explore seismic records, particularly in western Europe, to characterize the anomalies from Lop Nor. These anomalies include two aspects.

The first aspect is the recording of high-amplitude Love waves for almost all azimuths from Lop Nor. This aspect has previously been treated by *Zhang* [1994] and *Levshin and Ritzwoller* [1995]. They demonstrated that in the timedomain, significant Love waves are present for selected stations located at regional and teleseismic distances from the test site. Levshin and Ritzwoller also presented time-frequency images of the vertical and transverse components for two stations (AAK and GAR). This representation makes it possible to unequivocally identify the energy on the transverse components as Love waves but precise amplitude information is obscured by smearing in the time-frequency domain. We present further evidence of high-amplitude Love waves from Lop Nor by analysis of data from a larger number of stations and a better azimuthal coverage than previous investigations. Relative amplitudes of vertical, radial and transverse components are calculated as a function of frequency, paying particular attention to spectral amplitudes, as both tectonic release and path effects are expected to be strongly frequency dependent. The second aspect of the anomalies is an early Rayleigh wave as recorded by seismic stations in western Europe.

The station configuration that we use (Figure 1) is well suited for isolating different causes of the anomalies. Indeed, the Lop Nor test site, the former USSR test site of Semipalatinsk, the Russian station OBN in Obninsk, and broadband and long-period stations in France are all located close to on the same great circle. We can therefore compare records from explosions from the two test sites and unequivocally attribute anomalies from the Lop Nor test site observed in France to source effects or to path effects immediately north of Lop Nor. On the other hand, anomalies that appear between OBN and stations in western Europe must be due to path effects somewhere between OBN and western Europe.

The Lop Nor test site is located on the northern edge of the Tarim Basin, immediately south of the Tien Shan mountains and 300 km north of the plateau of Tibet. Figure 2 shows the altitudes and main faults in this area. Both the Tien Shan and Tibet are associated with thickened crust. The crust is up to 55 km beneath the Tien Shan [e.g., *Burov et al.,* 1990; *Avouac et al.,* 1993; *Kosarev et al.,* 1993; *Cotton and Avouac,* 1994] and up to 70 km beneath Tibet [e.g., *Gupta and Narain,* 1967; *Chen and Molnar,* 1981; *Hirn et al.,* 1984; *Brandon and Romanowicz,* 1986], while the crust beneath the Tarim Basin has an estimated thickness of 40 km [e.g., *Ma,* 1987; *Burov et al.,* 1990]. The explosions were carried out in the Paleozoic basement. The basement was affected by mainly thrust faulting during the Cenozoic, and it now forms alternate east-west striking ridges and intramontane basins filled with Cenozoic molasse [*Windley et al.,* 1990; *Allen et al.,* 1993]. These tectonics, related to the India-Asia collision [e.g., *Tapponnier and Molnar,* 1979], are ongoing and have induced an approximately north-south compression.

At Semipalatinsk (also known as the Shagan River test site) the detonations were also located in Paleozoic basement. The test site is located well north of the zone of active tectonics (Figure 2) but the stress field is probably similar to that around the Tien Shan and also characterized by a north-south compression [*Tapponnier and Molnar,* 1979]. *Ekström and Richards* [1994] show that the Love wave radiation is small to moderate for most explosions in Semipalatinsk. The similar stress fields at the two test sites indicate that if a much higher amount of tectonic release occurs for Lop Nor explosions, it cannot simply be due to the regional stress field but must be dependent on the presence of active deformation nearby. In terms of path effects, the main difference between the two sites with respect to seismic stations in western Europe is that surface waves from explosions in Lop Nor cross the Tien Shan mountains while those from Semipalatinsk do not cross any major active tectonic structures.

The Lop Nor test site is almost completely surrounded by areas with thickened crust. The influence in variation of crustal thickness on surface wave propagation is

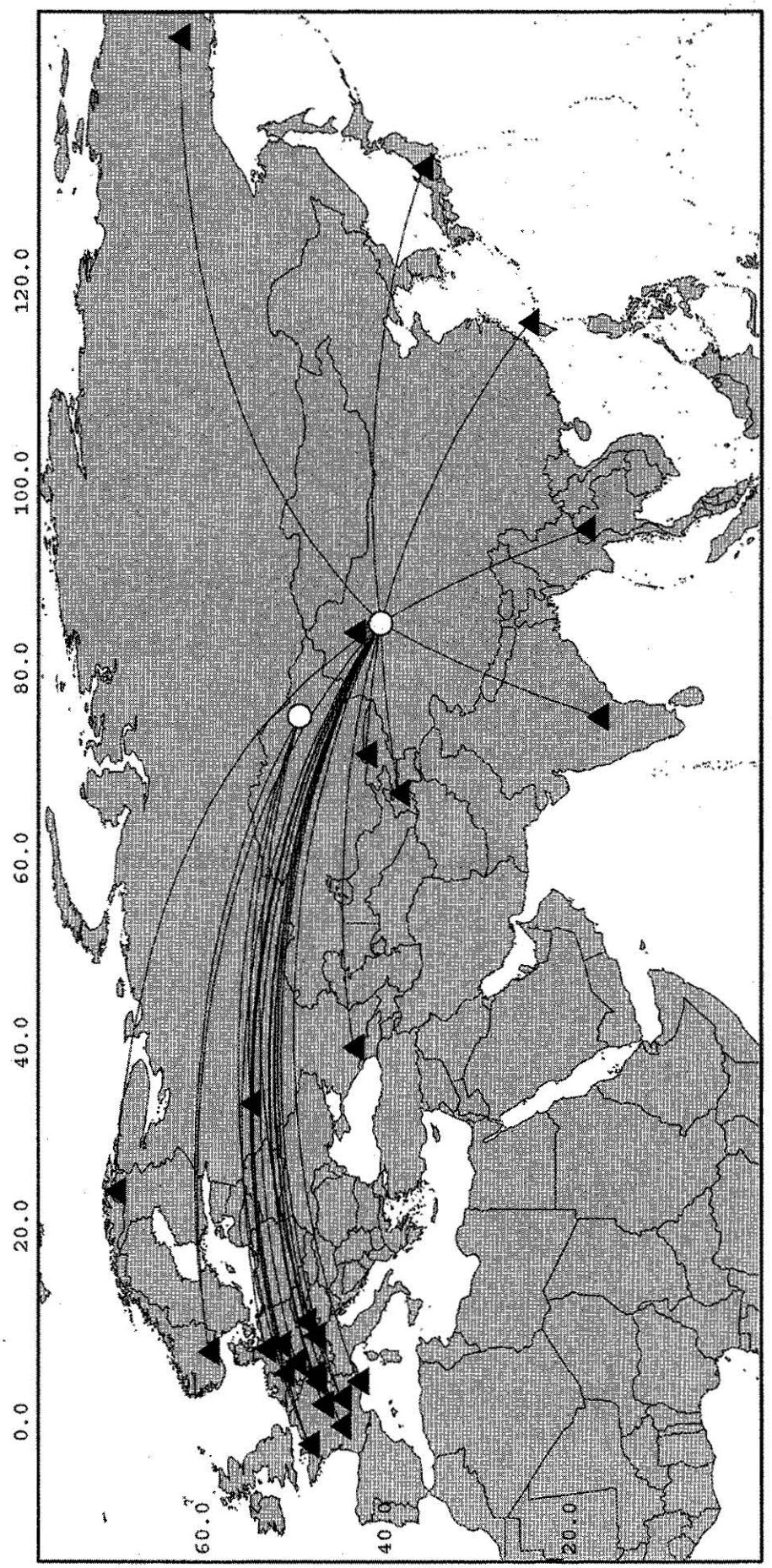

Figure 1. Stations used in the analysis. The stations in Germany and France are represented by station FLN. Great circle, solid and dashed lines; seismic station, triangle; nuclear test site, open circle.

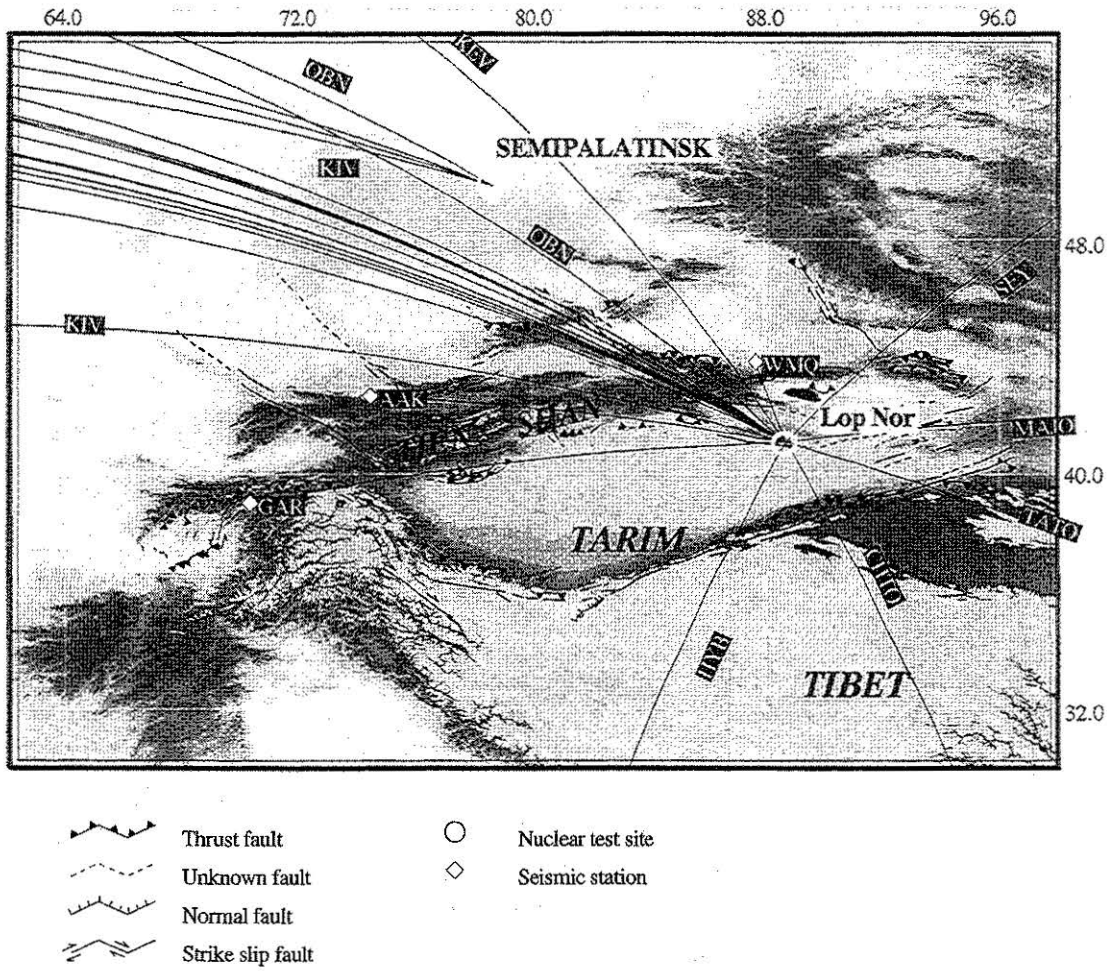

Figure 2. Tectonic setting of the Tarim Basin. The Lop Nor and Semipalatinsk test sites are shown by triangles, and great circles to stations are shown by lines.

therefore crucial in studying possible path effects on surface waves from Lop Nor. However, the effect of crustal thickening upon coupling between Love and Rayleigh waves is not easily assessed. Numerical simulations are necessary to quantify these diffraction effects, but most simulation methods that calculate surface wave propagation across laterally heterogeneous media take only smooth variations into account [e.g., *Snieder,* 1986; *Nolet,* 1990]. Strong lateral variations across boundaries separating two stratified half-spaces have also been considered (for a review, see *Its and Yanovskaya* [1985] and *Keilis-Borok,* 1989, and references therein]. Using the indirect boundary element method (IBEM) as presented by *Pedersen et al.* [1996], it is possible to calculate the complete wave field for surface waves incident on a strongly heterogeneous structure. IBEM is here used to estimate the Rayleigh-Love coupling across a thickened crust, using a simplified model of the Tien Shan.

In this paper we first describe surface waves from Lop Nor and Semipalatinsk as recorded by stations FLN and OBN. We next quantify the high Love wave amplitudes in the spectral domain and show how they vary when other stations located at varying azimuths from Lop Nor are considered. We next provide strong evidence for surface wave conversions at the Tornquist Zone. Finally, we present numerical simulations of Rayleigh-Love wave coupling across a simplified model of the Tien Shan, showing the influence of crustal thickening, the lower crustal structure, and the propagation direction on the coupling of Rayleigh and Love waves.

2. Observed Anomalies

Figure 1 presents the two test sites (Lop Nor and Semipalatinsk) and the seismic stations (long-period and broadband) used in this study. A large number of stations were located in France (the Laboratoire de Détection et de Géophysique (LDG) network and some GEOSCOPE stations) and Germany (the German Regional Seismic Network (GRSN)), supplemented by stations covering different azimuths as compared to the two test sites (data through Incorporated Research Institutions for Seismology (IRIS) and GEOSCOPE). The main focus in this study uses OBN and stations in northern Europe to estimate the location of the source of the observed anomalies.

Table 1. Coordinates and Magnitudes of the Events Used in This Study

Date yymmdd	Origin time UT	Latitude °N	Longitude °E	*Mb*
891019	09 49:57.3	49.90	78.97	5.9
920521	04 59:57.4	41.53	88.81	6.5
931005	01 59:56.7	41.63	88.69	5.9
940610	06 25:58.0	41.54	88.74	5.8

Three explosions (920521, 931005, and 940610) in Lop Nor and one in Semipalatinsk (891019) are used in the present study. Table 1 shows the characteristics of these four events.

Figure 3 shows traces of the 891019 detonation in Semipalatinsk and the 920521 detonation in Lop Nor, as recorded by stations OBN (Russia) and FLN (France). The traces are filtered between 10 and 100 s and displayed as a function of group velocity. This representation is not a common one, but it is an excellent means for comparing dispersive seismic waves at stations located at different epicentral distances. Note that this representation introduces an apparent dispersion of the waves, so the dispersion of the waves looks stronger than it is in reality. The traces are normalized so the relative amplitudes between vertical (Z), radial (R) and transverse (T) components are respected for each event and station, and so that the maximum amplitude on the Z component is the same in the four parts of the plot. The same type of normalisation is used for displaying the spectra and the frequency-time plots in the following subsections.

It is evident from this representation that records from the two events are significantly different. The

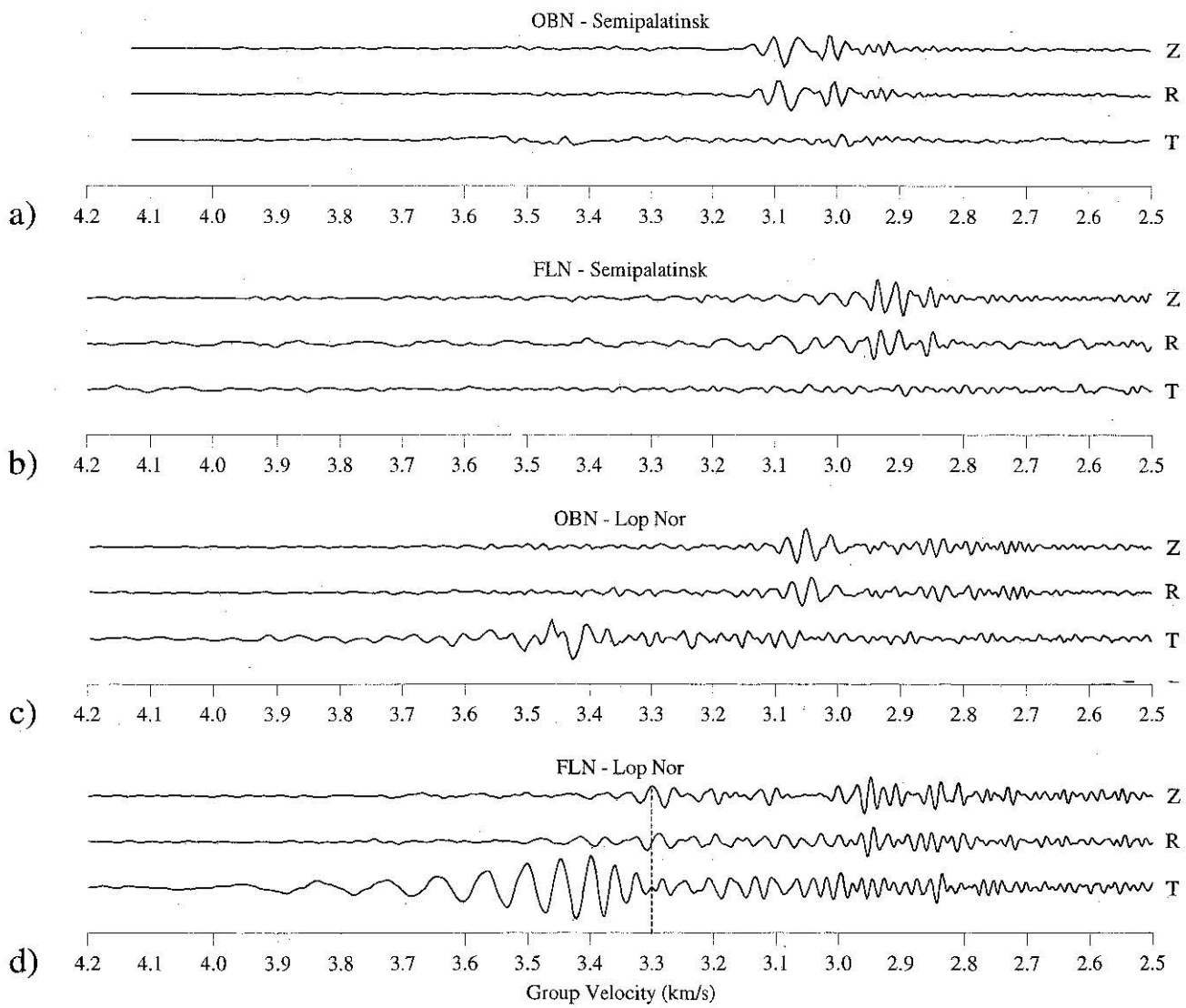

Figure 3. Band-passed (10-100 s) seismic records from stations OBN and FLN (a,b) of an explosion in Semipalatinsk and (c,d) an explosion in Lop Nor. The three components of motion (Z, vertical; R, radial, iT, transverse) are shown as a function of group velocity.

Semipalatinsk event shows hardly any energy on the transverse component, while the Lop Nor event shows strong, well-dispersed waves on the transverse component. These waves have a higher amplitude than the waves recorded for the radial and vertical components, and they are present both for stations OBN and FLN.

Another interesting feature is an anomalously early wave train (shown by a dashed line in Figure 3) of the vertical and radial components of waves from the Lop Nor event and recorded by FLN. This early wave train is not present on the records from OBN. In the following two subsections we investigate these two anomalies in more detail using other explosions and stations.

2.1. Anomalously Strong Love Waves From Lop Nor

To determine whether Rayleigh waves as observed at stations OBN and FLN are particularly attenuated for the Lop Nor event, the spectra of the records shown in Figure 3 were corrected for geometrical spreading and divided by 10^{Mb} to correct for differences in yield. Considering the uncertainty of *Mb* as reported in the bulletins, we cannot determine with certainty whether the Rayleigh waves are attenuated for the Lop Nor event, even though some attenuation seems to be present. Consequently, we concentrate on relative amplitudes of the three components at various locations.

To systematically determine the amplitude anomaly of the transverse component as compared to the radial and vertical components and as a function of frequency, we analyzed records from broadband and long-period stations located at different azimuths from the Lop Nor test site. The stations, sorted by increasing azimuth, are SEY, MAJO, TATO, CHTO, HYB, GAR, AAK, KIV, OBN, FLN, KONO, and KEV (see Figure 1). Figure 4 shows the spectra of vertical (dotted lines), radial (dashed lines), and transverse (solid lines) components for these stations (time filtered between 2.5 and 4.2 km/s group velocities). The observed data were corrected for offset and trend and a cosine taper was applied prior to the calculation of the spectra. As we here focus on the relative amplitudes of the three components, the spectra were normalized independently for each station with respect to the maximum spectral amplitude of the vertical component. For some stations there were slight differences (due to a constant amplitude factor) in station response for the three components. This was corrected for, but to avoid instabilities at low frequencies, the signals were otherwise not deconvolved by the station response. For each of the stations, the azimuth, back azimuth, and the distance to Lop Nor are shown. The spectra are shown on a log-log scale to enhance the intermediate period range and to have sufficient dynamics on the amplitude axis.

Significant energy is present on the transverse component at all stations. One can separate the anomalies into three types. For 7 of the 12 stations ("type 1": SEY, TATO, HYB, AAK, KIV, OBN, and FLN), located at azimuths between 38° and 310°, the transverse component in a frequency interval between approximately 0.015 and 0.045 Hz is of several times higher amplitude than the vertical component. Above 0.045 Hz, the scatter is somewhat higher, but the transverse amplitude is at least of the same order as that of the two other components. For three stations ("type 2": MAJO, GAR, and KONO), located at azimuths 81°, 266°, and 320°, the amplitude of the transverse component between 0.015 and 0.045 Hz is equal to or slightly higher than that of the other components. Finally, for two stations ("type 3": CHTO and KEV), located at azimuths 156° and 333°, the amplitude of the transverse component is smaller than that of the other components up to approximately 0.035 Hz. The amplitudes are approximately the same above this frequency. The data from station WMQ (azimuth 345°) are not available although data from one Lop Nor explosion is published for this station (also referred to by *Levshin and Ritzwoller*, [1995]). WMQ is located too close to Lop Nor for the intermediate to long-period surface waves to be well developed, but it seems to be of type 3, that is, the same as its "neighbor", KEV.

In Figure 4 it is intriguing that stations located at azimuths differing by approximately 180° have comparable amplitude ratios between the transverse and the other components. This could indicate a source effect. However, for this hypothesis to be valid the radiation pattern must be identified in the absolute amplitudes. We therefore calculated absolute amplitudes (corrected for instrument response and geometrical spreading) for the 12 stations. Figure 5 shows the vertical (crosses) and transverse (circles) corrected amplitudes at two different periods (20 and 40 s) as a function of azimuth in polar plots. The absolute amplitudes vary highly as a function of azimuth. Even though some of this scatter can be attributed to the use of a single frequency, the spectra are sufficiently smooth (at least at 40 s period; see Figure 4) for the scatter to be representative of the real scatter in amplitude as observed in data. If the amplitude anomalies are purely due to tectonic release, the transverse amplitudes should show a simple radiation pattern (dependent on the sine of the azimuth or twice the azimuth). The station density towards the northwest is sufficient for us to be confident that there is no simple radiation pattern present in the amplitudes represented in Figure 5.

Normalized spectra of three different explosions in Lop Nor recorded at OBN are shown in Figure 6. The spectra are shown only in the intervals where the signal-to-noise ratio was good. For each event, the amplitudes of the spectra were normalized by the average energy of the vertical component between 0.02 and 0.05 Hz. The shape of the spectra for each component is very similar when different events are compared, indicating that the seismic sources are very similar. Whatever cause is suggested for the high Love wave amplitudes, it must also account for this similarity between sources.

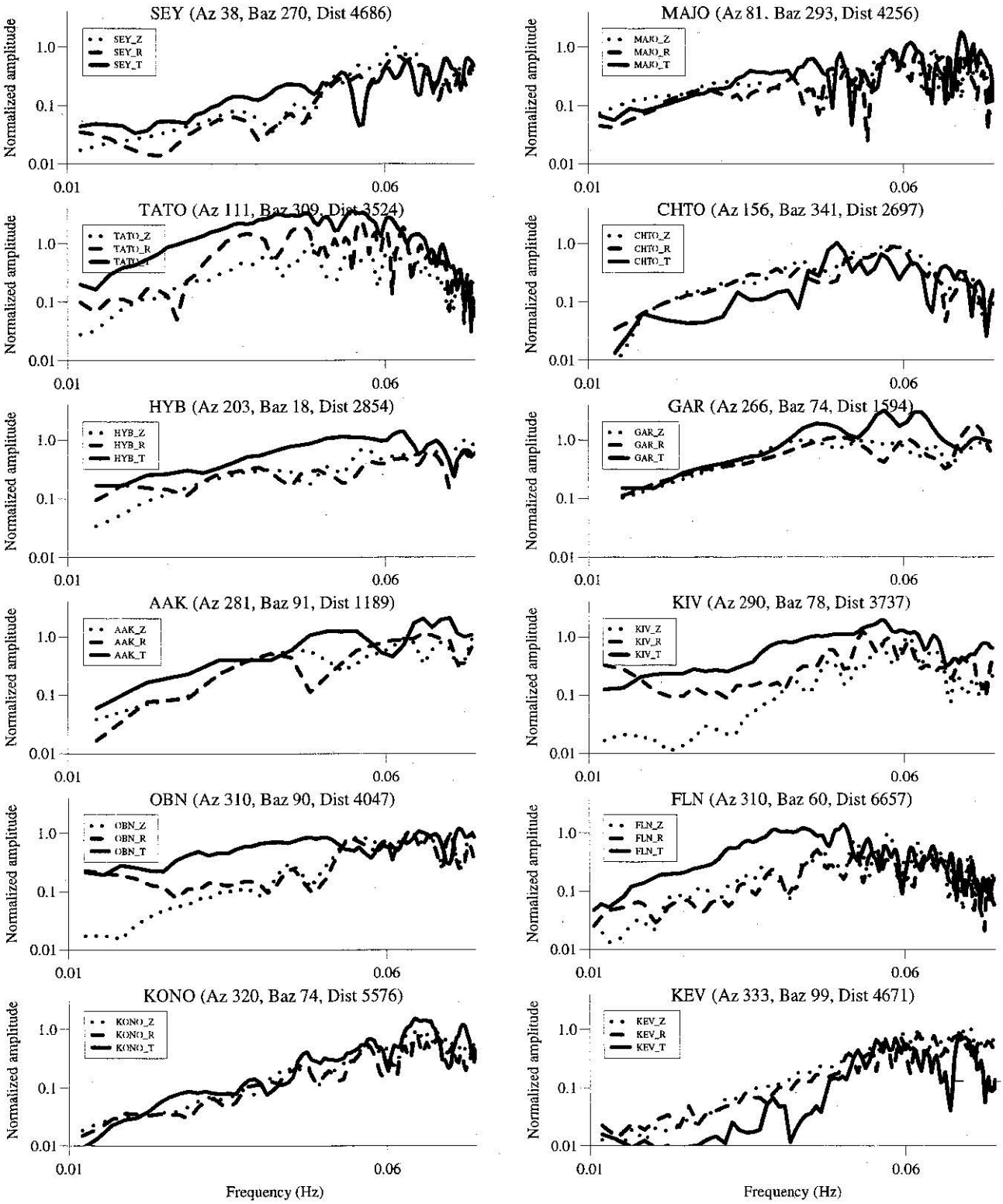

Figure 4. Spectral amplitudes for stations located at different azimuths and distances from Lop Nor. In each plot the transverse component is shown by the solid line, the radial component by the dashed line, and the vertical component by the dotted line. The station name, the azimuth, back azimuth, and distance are annotated onto each plot.

We performed a frequency-time analysis to verify whether the energy on the transverse components observed at OBN and FLN is mainly of Love waves. We used the multiple filtering analysis [*Dziewonski et al.*, 1969; see also *Keilis-Borok*, 1989]. This type of analysis yields energy diagrams in the time-frequency domain (that we have transformed to group velocities and periods) in which group velocity dispersion can be selected

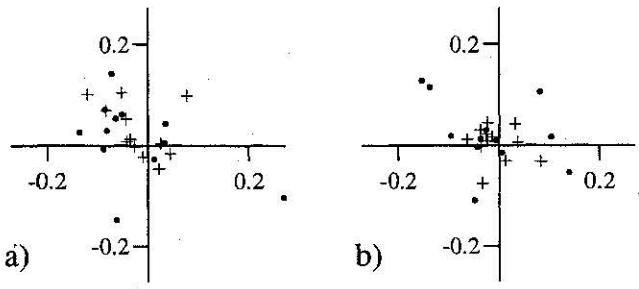

Figure 5. Spectral amplitudes corrected for geometrical spreading as polar plot. (a) 20 s period and (b) 40 s period. Vertical component, crosses; transverse component, circles. The unit is $m^{3/2}$.

as the curve through the amplitude maxima. The amplitudes are again normalized with respect to the vertical component. In this type of filtering, it is important to be aware of the trade-off between the time and frequency resolution, which introduces "smearing", and the amplitudes shown in the figures depend somewhat on the filters chosen in the analysis.

An example of such an analysis (for event 920521, station FLN) is shown in Figure 7. To facilitate the estimation of the differences between the energy diagrams of different components, we also show "theoretical group velocity curves" (Rayleigh waves, solid line; Love waves, dashed line) in Figure 7. The theoretical Rayleigh wave dispersion is the average dispersion curve on the vertical component between Semipalatinsk and several long-period and broadband stations in France. The Rayleigh wave group velocities between Lop Nor and France must lie close to this curve because most of the propagation path between Lop Nor and France is very close to the path between Semipalatinsk and France. The theoretical Love wave dispersion curve is obtained by first inverting for the average Earth structure that corresponds to the Rayleigh wave dispersion curve and second calculating the Love wave dispersion curve for this Earth model. These curves are not inter-

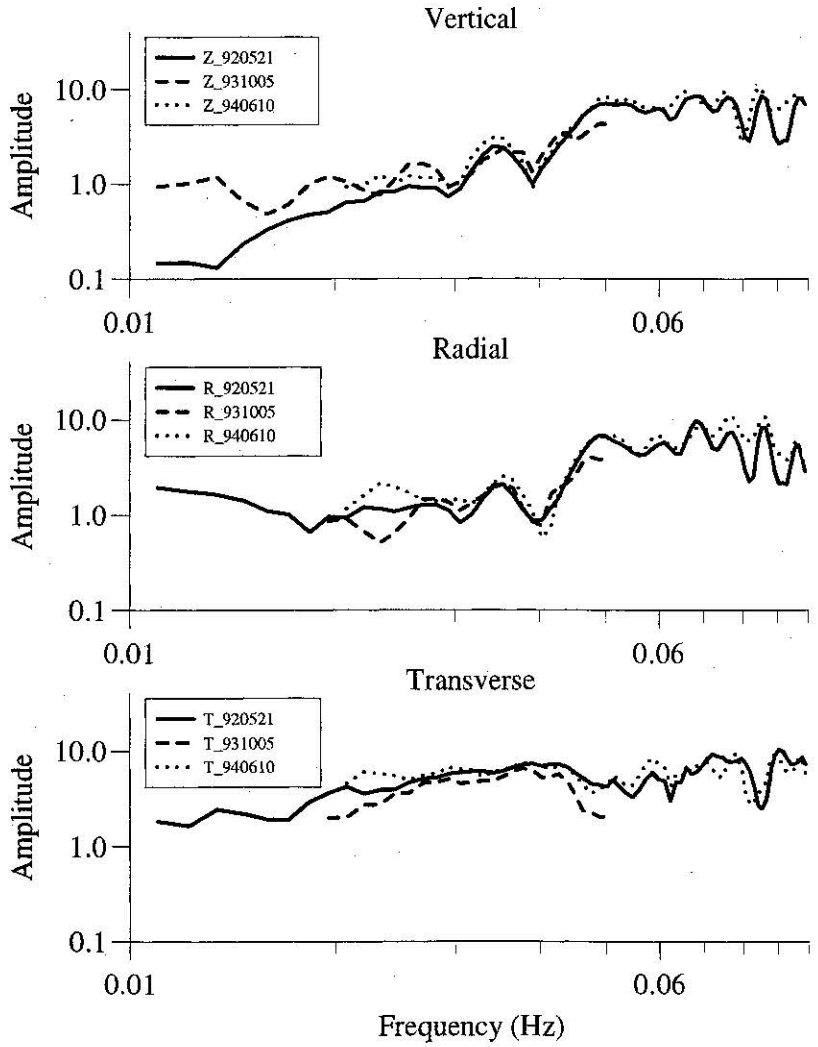

Figure 6. Spectra of three different explosions in Lop Nor recorded at OBN. The three explosions are annotated by the year, month, and day of the event. For each event the amplitudes of the spectra are normalized by the average energy of the vertical component between 0.02 and 0.05 Hz.

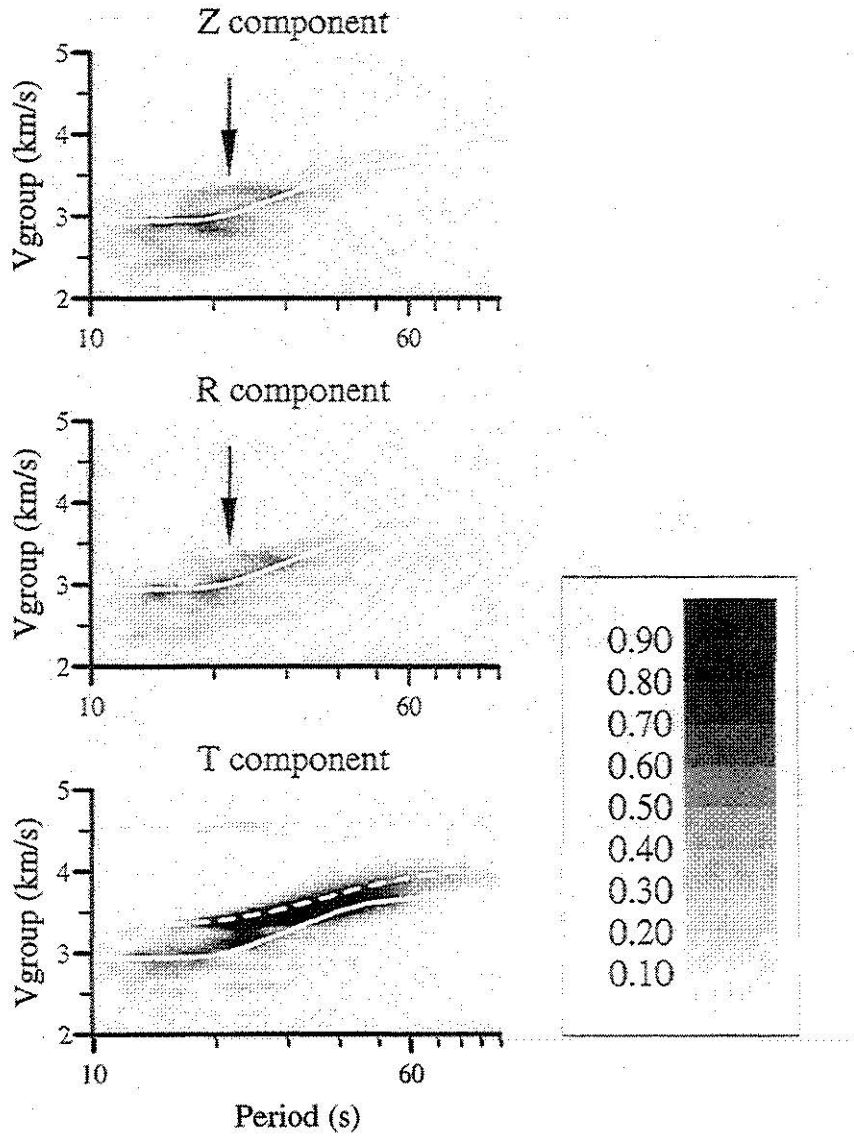

Figure 7. Result of multiple filter analysis on records from FLN. The plots are normalized so that the maximum amplitude is one for the vertical component. The "theoretical dispersion curves" as discussed in the main text are shown for the Love waves (dashed line) and the Rayleigh waves (solid line). The anomalous early wave train is shown by arrows for the vertical and radial components.

preted in this paper but are simply used to ease identification of Love and Rayleigh waves in the energy diagrams. The high amplitudes on the transverse component can clearly be identified as Love waves (Figure 7). Furthermore, a strong coda is present on all components for periods shorter than 30 s.

2.2. Anomalous Early Arrivals in France and Germany

In the frequency-time diagram there seems to be anomalously high level of energy present on the vertical and radial components between 20 and 30 s period and for a group velocity of approximately 3.3 km/s (Figure 7 at the arrow). This energy corresponds to a distinct wavelet on the seismic records of FLN at a group velocity of 3.3 km/s (Figure 3, at the dashed line). The early wave train is addressed in more detail in this subsection.

Figure 8 shows the seismic broadband and long-period stations in France and Germany. Frequency-time analysis shows that the early wave train is present with significant amplitude at the seven stations in France and at four out of the six stations in Germany (BUG, TNS, WET, and FUR), while it is absent at OBN and KONO. The exact arrival time, frequency content, and amplitude of the wave train is difficult to estimate in the time-frequency plot, but the wave train clearly arrives earlier than expected for the Rayleigh waves. At HAM and CLZ there is some early energy in the frequency-time diagram, but the amplitude is very small. Out of the six GRSN stations, HAM and CLZ are the two northernmost ones (Figure 8).

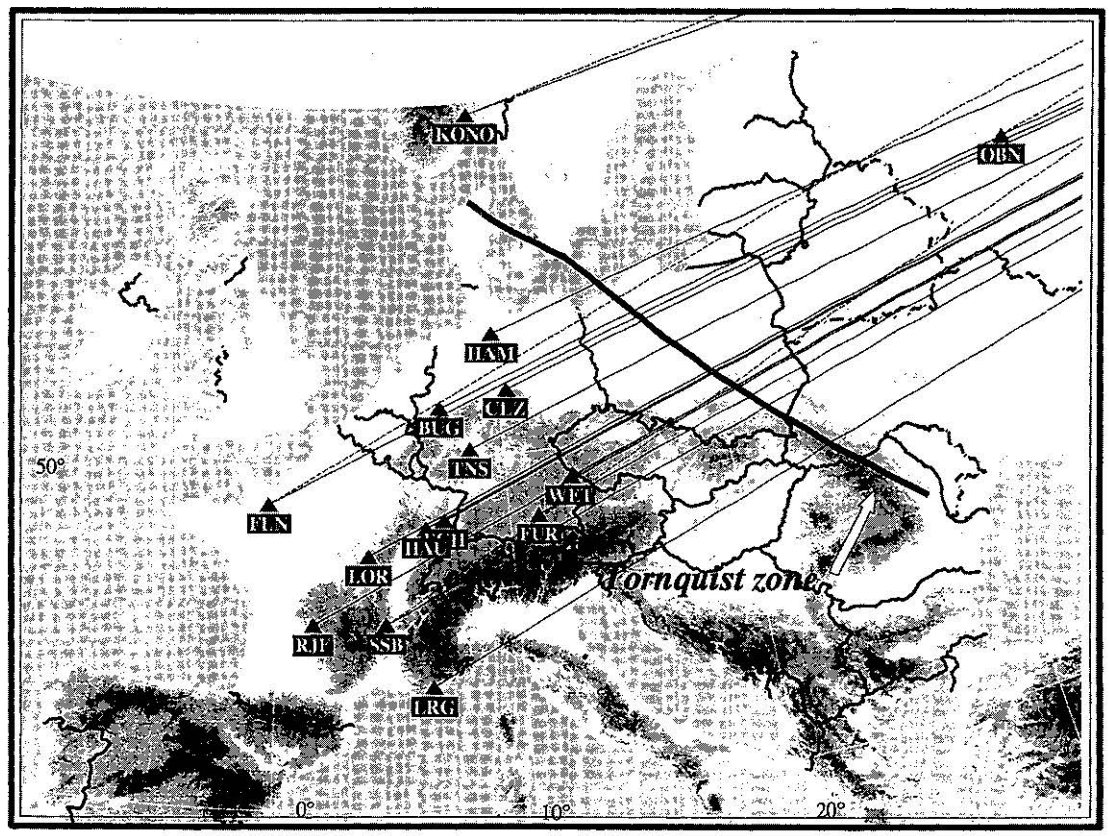

Figure 8. Map of the long-period and broadband stations from France and Germany used in this study. Triangles, seismic station; solid line, great circle from Lop Nor; dashed line, great circle from Semipalatinsk.

Figure 9 shows the particle motion in the radial-vertical plane at FLN in a time window delimited by the group velocities 3.25 and 3.35 km/s. This particle motion shows that the early wave train has the polarization of a Rayleigh wave.

To estimate the azimuth of the early wave train, a simplified array analysis was performed on the records from France. For each station, the arrival time was estimated by measuring the time of maximum envelope of the signal between 3.2 and 3.5 km/s after a narrow band-pass filtering (corner frequencies 0.03 and 0.07 Hz). We estimate the precision of this measurement to be approximately 1 s. We calculated the observed delay $\delta_{o,k}$ at each station k as the difference of the observed arrival times at the station and at ECH.

Under the assumption that the incoming wave is plane, with a propagation direction θ ("wave back azimuth") from the north and constant velocity V, the variance χ of the difference between the theoretical and observed delays can be calculated as

$$\chi = \sqrt{\frac{1}{N-1}\sum_{k=1}^{N}\frac{(\delta_{o,k}-\delta_{t,k})^2}{\sigma_k}}$$

where $\delta_{o,k}$ is the observed delay for station k, $\delta_{t,k}$ is the theoretical delay for station k (for a given V and θ), N is the number of stations, and σ_k is the uncertainty of the estimation of the observed delay at station k. The uncertainty of the time of the maximum peak of the envelope is approximately 1 s, so the uncertainty on the observed arrival time difference $\delta_{o,k}$ can be estimated to

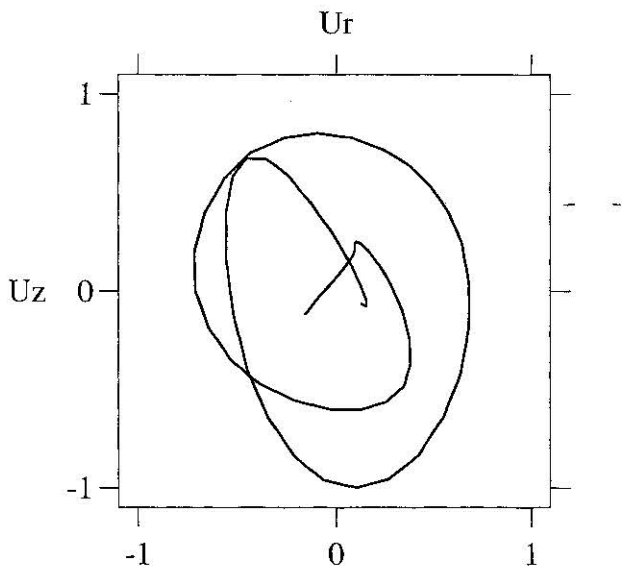

Figure 9. Particle motion of the early wave train, as recorded at FLN after band pass filtering 10 to 100 s. The amplitudes are normalized so the maximum amplitude of the vertical component is 1.

2 s for all stations. Even though the amount of data is too small to perform a proper statistical analysis, at the first approximation solutions are acceptable for (V,θ) for which χ is smaller than 1. Figure 10a shows log(it χ) as a function of V and θ. Variable $\log(\chi)$ is used in the figure rather than χ to increase the clarity and dynamics of the color coding. Acceptable values of V and θ correspond to negative values (black color coding) in the plot. The values of θ and V are acceptable only in a very narrow interval. χ is minimized with $\theta = 63^0$ and V=2.625 km/s. Using these two values, the fit between theoretical and observed time delays is very good, as can be seen in Figure 10b. Observed and theoretical time delays are plotted as a function of the distance of the station to ECH as projected on 63°N through ECH.

A propagation direction of 63°N corresponds to the theoretical back azimuth of the explosions in Lop Nor as observed in France, and 2.63 km/s corresponds approximately to the Airy phase (at 2.75 km/s) of Rayleigh waves in a simple crustal model of France [*Perrier and Ruegg*, 1973].

The velocity, direction of propagation, and polarization of the early wave train are strong indications of a Rayleigh wave. The existence of a Rayleigh wave so early in the records points towards a partial Love to Rayleigh conversion somewhere northeast of the stations in south and central Germany. A likely candidate for such a wave conversion is the Tornquist Zone, which is associated with changes in crustal thickness and upper mantle anomalies [*Guterch et al.*, 1986; *EUGENO-*

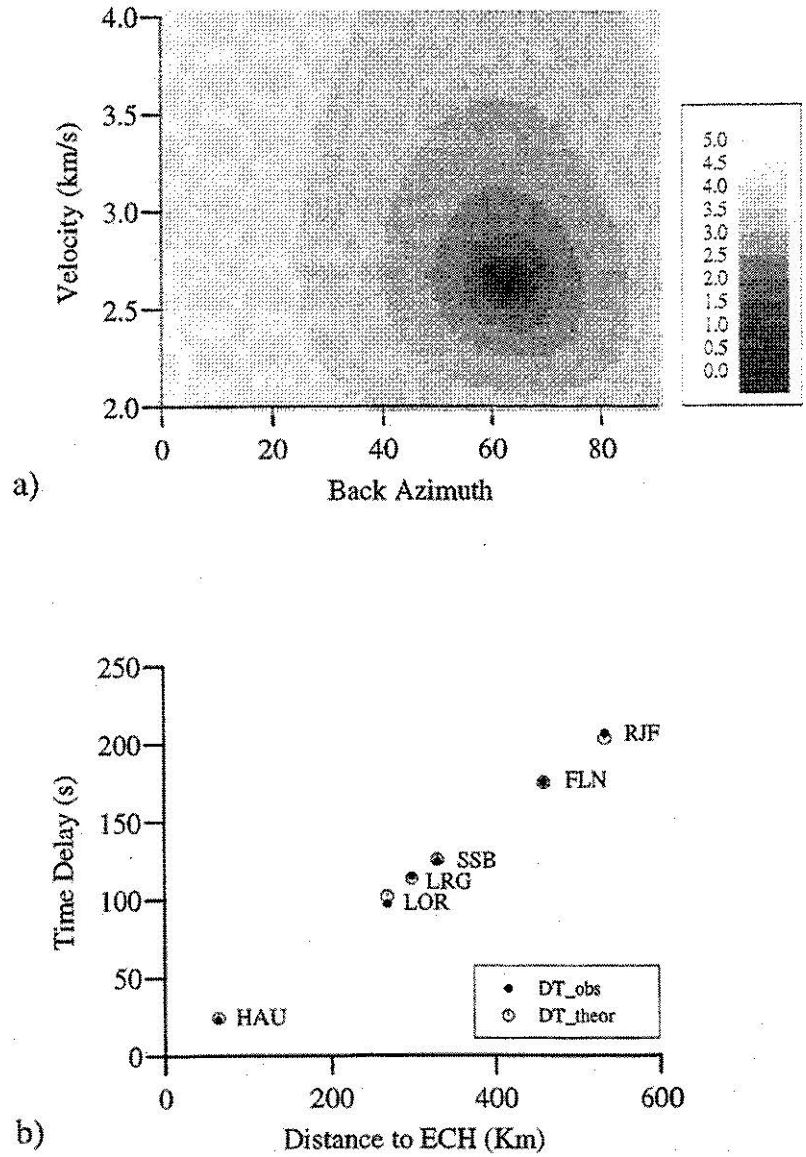

Figure 10. Determination of arrival angle and velocity of the early wave train. (a) Variable $\log((\chi)$ as a function of back azimuth and velocity. We refer to the main text for the definition of χ. (b) Theoretical (open circles) and observed (solid circles) delay times of the early wave train between the different stations in France and ECH. The theoretical delays are calculated by assuming a plane wave crossing the area with a velocity of 2.63 km/s and a wave back azimuth of 63°. The delays are shown as a function of the distance between the stations and ECH, as projected on a line striking 63°N.

S Working Group, 1988; *Pedersen et al.,* 1994; *Zielhuis and Nolet,* 1994]. To estimate whether the location of the wave conversion at the Tornquist Zone is compatible with the observations in terms of travel time and propagation velocities, we performed a simple and approximate analysis. Neglecting refraction effects, the observed arrival time at station k of the early wave train $t_{o,k}$ is

$$t_{o,k} = \frac{\Delta_{1,k}}{V_L} + \frac{\Delta_{2,k}}{V_R}$$

where $\Delta_{1,k}$ is the distance on the great circle (passing through Lop Nor and the station) between Lop Nor and the Tornquist Zone, and $\Delta_{2,k}$ is the distance between the Tornquist Zone and the station, V_L is the Love wave velocity (assumed to be constant) east of the Tornquist Zone, and V_R is the Rayleigh wave velocity west of the Tornquist Zone (assumed to be constant at 2.63 km/s). For each station, we can therefore estimate the Love wave velocity east of the Tornquist Zone. We obtain an average V_L of 3.53 $\pm$0.02 km/s. On our theoretical Love wave dispersion curve (e.g., Figure 7), this velocity corresponds to approximately 29 s period, which is compatible with the period of the observed early wave train. This analysis therefore indicates that a Love-Rayleigh wave conversion at the Tornquist Zone is compatible with the arrival times of the early wave train as observed in France.

2.3. Summary of Observations and Interpretations

The teleseismic records from the 920521 Lop Nor explosion show a very consistent surface wave anomaly: Love waves that are of at least the same amplitude as the Rayleigh waves, and in most cases higher, for almost all azimuths. This amplitude anomaly is strongest between 0.015 and 0.045 Hz. The same amplitude anomaly is not only present in records from the strong 920521 explosion, it is present for other Lop Nor events as well. The similarity of spectra from Lop Nor explosions with different yield (Mb=5.8-6.5) is an indication of very similar source mechanisms and source time functions.

The early wave train observed at stations in France is an indication that conversions between Love and Rayleigh waves can be strong in some cases. On that particular phase the Tornquist Zone was identified as the most likely location of wave conversion. The opposite effect, Rayleigh to Love wave coupling, may be a partial explanation for the observed Love wave anomalies associated with the Lop Nor explosions. The following section therefore focuses on numerical simulations of path effects to investigate more closely the parameters which influence conversions between Rayleigh and Love waves.

3. Numerical Simulations

We intend to investigate to what extent path effects can account for the observed anomalies. Our main interest here is the partial conversion between Rayleigh and Love waves which takes place at lateral heterogeneities. To produce strong Rayleigh to Love wave coupling, the lateral heterogeneities must be strong, that is, with strong lateral contrasts in elastic parameters. The wave propagation must also be three-dimensional (3-D), that is, either the heterogeneities are of 3-D geometry or they are of 2-D geometry with surface waves incident outside the 2-D plane.

We use the indirect boundary element method adapted to surface wave propagation in multilayered media [*Pedersen et al.,* 1996] to simulate plane surface waves obliquely incident upon a 2-D structure. This type of diffraction is sometimes named "2.5-D diffraction," which is somewhat misleading because the wave propagation is 3-D with coupling of all wave types. IBEM has the advantage to calculate the total wave field (with all wave conversions included) and to accommodate very strong lateral changes in elastic parameters. The simulations are carried out in the frequency domain, consequently synthetic seismograms are obtained by multiplication with a source function followed by an inverse Fourier transform.

Ideally, we would simulate waveforms at the different station locations, taking into account all the known lateral heterogeneities located in a large region around the great circle path. This is unfortunately too demanding in terms of computer memory and CPU time due to the relatively high frequencies and the need to solve the full wave equation. We therefore instead aim at a qualitative understanding of the influence of the type of lateral heterogeneities which are known to exist in proximity of the Lop Nor test site.

3.1. Models

In terms of its large-scale structure, the main characteristic of the Tarim Basin is that it is surrounded by areas with significant crustal thickening (Figure 2). The crust is probably up to 55 km thick beneath the Tien Shan mountains towards the north and west, and up to 70 km beneath Tibet towards the south. The surface waves emitted from Lop Nor must therefore cross a thickened crust for almost all azimuths. We consequently study Rayleigh to Love wave conversions across a crustal thickening.

We choose to simulate Rayleigh to Love wave conversions across the Tien Shan for the following reasons. First, in spite of lateral variations [e.g., *Roecker et al.,* 1993], the Tien Shan can in most places locally be approximated by a 2-D structure. This is not the case for Tibet, where the local structures and Moho depth vary significantly even within the plateau [e.g., *Wittlinger et al.,* 1996] and are largely unknown. Second, the main part of our data set comes from stations for which the recorded Rayleigh waves have crossed the Tien Shan mountains. Finally, the structure along the great circles between Lop Nor and the stations in Europe is significantly simpler than for waves that are recorded by

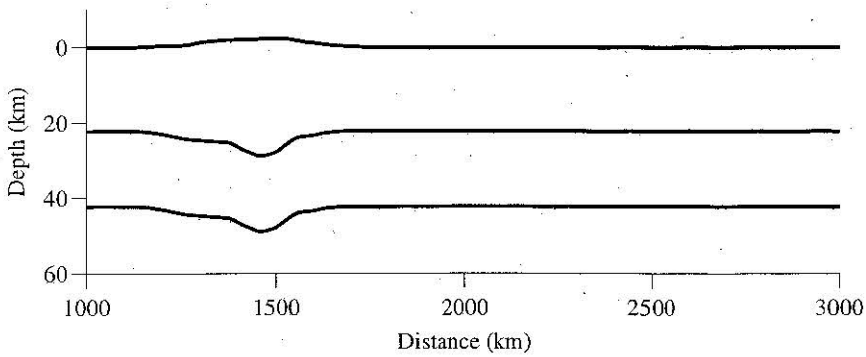

Figure 11. Model 1 of the Tien Shan (tenfold vertical exaggeration), as used in the numerical simulations. Each layer is homogeneous, but the depth of the interfaces vary across the model.

stations located towards the south and east. If significant wave conversions occur across a Tien Shan model, it is likely that similar or even stronger wave conversions can occur towards the south and southeast, depending on the precise path of the surface waves, their angle of incidence upon the heterogeneities, etc.

The main problem in the simulation is that Lop Nor is located very close to the Tien Shan mountains, so long-period wave diffraction occurs in the near field to the source, and the waves incident upon the Tien Shan are not plane and these effects are not taken into account in the simulations. The effects of a near-field diffraction as compared to diffraction of plane Rayleigh waves is difficult to assess. The simulations nevertheless make it possible to determine which parameters control the surface wave diffraction, whether wave conversions are likely to be significant, and in which frequency intervals such conversions occur.

To be able to study the influence of different model parameters on the diffraction, we use a simple crustal model of the Tien Shan in the numerical simulations. This crustal model is based on *Burov et al.* [1990], *Avouac et al.* [1993], *Kosarev et al.* [1993] and *Cotton and Avouac* [1994].

In the first model, shown in Figure 11, the crust is assumed to be 42 km thick on each side of the range, and up to 49 km thick beneath it. The lower crust is 20 km thick across the whole model. The elastic parameters of the model are shown in Table 2. The range is located between 1100 km and 1800 km, that is, over a width of 700 km. However, the area of significant crustal thickening is only 300 km wide. We discuss the simulations based on this model (model 1) in some detail as it is used as a reference in further simulations.

Table 2. Elastic parameters used in the numerical simulations

Unit	Vp km/s	Vs (km/s) km/s	ρ g/cm^3
Upper crust	6.5	3.9	2.60
Lower crust	7.0	4.0	2.75
Mantle	7.9	4.9	3.35

A fundamental model Rayleigh wave is incident upon the structure with an azimuth ϕ. The azimuth is defined as the angle between the propagation direction of the incident Rayleigh waves and the direction perpendicular upon the structure. An azimuth of 0° therefore corresponds to waves perpendicularly incident on the structure (and hence purely 2-D propagation with no Rayleigh-Love wave coupling), and an azimuth of 90° corresponds to Rayleigh waves arriving parallel to the strike of the structure.

3.2. Results of Numerical Simulations

Figure 12 shows the synthetic seismograms for a plane fundamental mode Rayleigh wave incident on the model with 30° azimuth. The ground displacement is simulated at 101 points at distances between 1000 and 3000 km. These distances refer to the distances of the model as shown in Figure 11, that is, perpendicular to the structure. The lateral extension of the crustal thickening is shown by a thick line on the distance scale. The source function is a Ricker wavelet with a 20 s central period. The displacements are shown in the vertical (Z), radial (R), and transverse (T) coordinate system.

In the flat-layered parts of the model, the Love and Rayleigh waves propagate independently, and as the layer thicknesses are the same on each side of the range, the fundamental mode Rayleigh waves are purely in the radial-vertical plane. The transverse component far behind the range (for large distances) can therefore be identified mainly as Love waves, even though some of the Love wave energy is on the radial component due to refraction effects. However, even far behind the range, the amplitudes on the transverse components change somewhat with distance.

The shape and amplitude of the spectra change significantly across and on the far side of the range. It is not possible here to show all the spectra, so the following figures are selected for illustration.

Figure 13 shows the spectral amplitudes at the distances x=1000 km (i.e., on the side where the Rayleigh waves are incident) and x=2500 km. The Rayleigh to

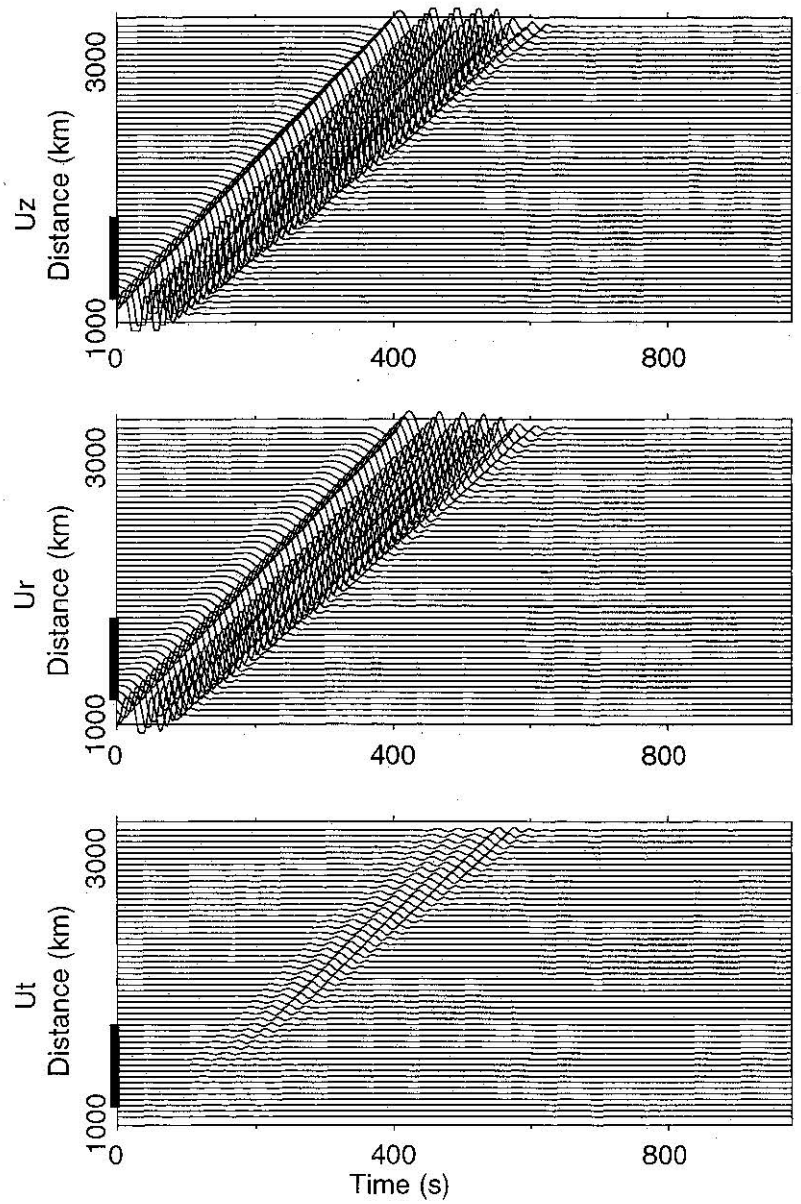

Figure 12. Time plots of the numerical simulations of a fundamental mode Rayleigh wave incident on the Tien Shan. The source function is a Ricker wavelet with a central frequency of 0.05 Hz. The thick line corresponds to the area with crustal thickening.

Love wave conversions take place from frequencies of approximately 0.02 Hz, which coincide well with the observed anomalies (section 2.1). The Love wave spectrum at 2500 km is rather smooth, while the Rayleigh wave spectrum shows a significant trough above 0.05 Hz with a minimum at 0.085 Hz. The existence of spectral peaks and troughs on the vertical and radial components is also qualitatively in agreement with the observations (see Figures 4 and 6). The trough is due to the interaction between the "primary" Rayleigh wave emitted from the source and several other waves. These other waves are "secondary" fundamental and higher mode Rayleigh and body waves which are created by wave diffraction across the structure. The relatively simple lithospheric structure of the model leads to the interference of only a limited number of direct and converted waves. In reality, the lithosphere is of 3-D geometry and more heterogeneous than assumed in the model, consequently other converted waves may be generated, and this may explain why observed surface waves have more complex spectra with many peaks and troughs.

Due to the spectral troughs, the transverse/vertical spectral amplitude ratio can be high at selected frequencies. For example, the spectral ratio between the transverse and vertical component at 2500 km is 4.9 at 0.085 Hz due to the spectral trough on the vertical component. Due to the interaction between different waves, the frequency locations of the spectral troughs vary as a function of distance and are very dependent on the model. In observed data, the spectral troughs will never be as deep as shown here because real wave fields are more complex than the single-mode Rayleigh waves used here. To focus on the amplitude of the Love waves rather than on the spectral troughs in the

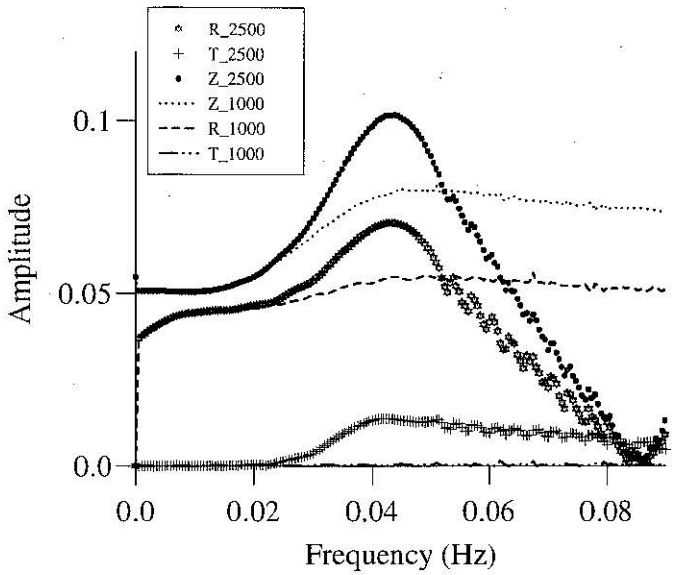

Figure 13. Spectral amplitudes of the vertical, radial, and transverse component at distances x=1000 km and x=2500 km for incident Rayleigh waves on model 1. The legend to the right identifies the spectra by the first letter (the component) and the number (the distance).

Rayleigh waves, Love wave amplitudes are in the following figures represented by the spectral ratio between the transverse component at 2500 km and the vertical component at 1000 km.

Note, however, that this spectral ratio will generally be lower than the ratio between the transverse and the vertical components (both measured at 2500 km) which would be expected in observed data because the attenuation of the Rayleigh wave across the crustal heterogeneity is not taken into account. Also note that the Love waves propagate with an angle other than 30° to the structure because the Love wave propagation velocity is different to that of the fundamental mode Rayleigh waves. This again leads to an underestimation of the Love wave amplitudes. These two effects can probably at the most lead to an underestimation by a factor of 2 of the amplitudes of Love versus Rayleigh waves.

Figure 14 shows the Love wave amplitudes for simulations with Rayleigh waves incident on model 1 with azimuths ranging from 10° to 50°. At 0° azimuth the Love wave amplitude is 0. An azimuth increase generally induces an increase in Love wave amplitudes. The amplitude increase for a 10° azimuth increase is higher for low than for high azimuths. The frequency for which the Love wave amplitudes is maximum is also somewhat dependent on the azimuth, but the overall shape of the spectra remains the same for all azimuths. The increase of amplitude with azimuth shows that Love waves observed on the far side of a thickened crust (relative to the seismic source) can have an apparent radiation pattern simply due to the azimuth dependence of the surface wave conversions. This result could explain the decrease of the observed transverse/vertical ratio from stations KONO, PLN, and OBN to stations KEV and WMQ by the decrease of azimuth of the incoming waves upon the Tien Shan.

A large number of simulations were carried out changing a single parameter at a time. The main conclusions of this parametric study are the following:

1. The surface topography alone only has a minor influence on the conversion of Love waves. The surface topography is too small to significantly influence the surface waves at the wavelengths considered here. 2. The precise geometry of the crust-mantle interface as well as the thickness of the lower crust has a minor influence on the amount of converted Love waves. 3. The difference in crustal thickness between the range and the surrounding regions has a strong influence on the amount of converted Love waves: the greater the difference in crustal thickness the stronger the Love wave generation. 4. Introduction of a low-velocity layer in the crustal root enhances Love wave conversion.

These results are not surprising, because greater Love wave amplitudes are expected with increasing lateral heterogeneity. For illustration, Figure 15 shows Love wave amplitudes for model 1 and for two other models. The main parameters of the three models are shown in Table 3. In model 2 the crustal thickening is increased to 18 km (assuming a crustal thickness of 37 km in the Tarim Basin and 55 km beneath the range). In model 3 the crustal thickening is 18 km, and it is characterized by a low-velocity layer in the crustal root. The top of the low-velocity layer is flat and located at 37 km depth. The wave velocities are 6.5 km/s for P waves and 3.5 km/s for S waves in the crustal root. In all three simulations, the azimuth of the incident Rayleigh waves is 30°.

The maximum amplitudes of the transverse component are generally greater (by up to 25%) in model 3 than in model 2. However, this is somewhat variable

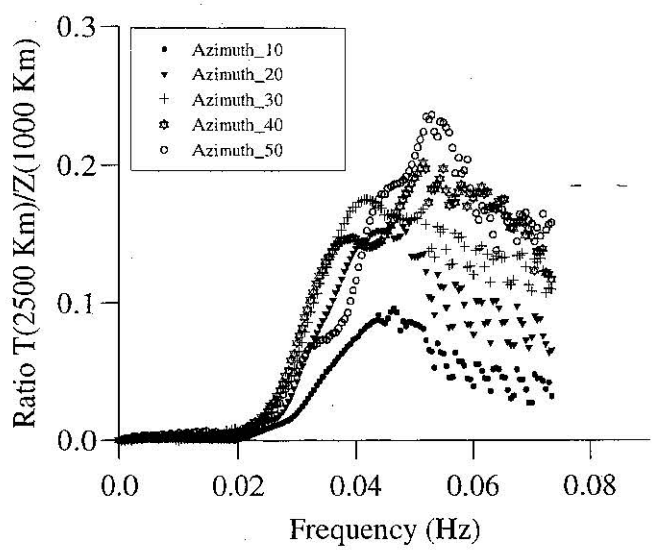

Figure 14. Spectral ratios of the transverse component at x=2500 km over the vertical component at x=1000 km for five different azimuths: 10°, 20°, 30°, 40°, and 50°, and for an incident Rayleigh wave on model 1.

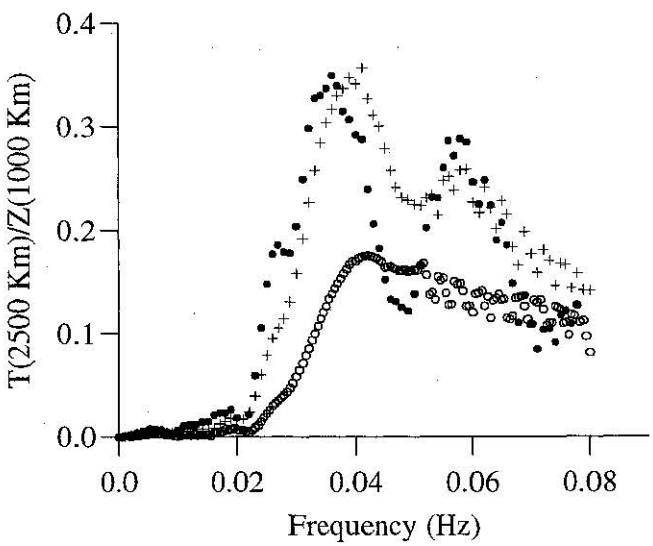

Figure 15. Spectral ratios of the transverse component at x=2500 km over the vertical component at x=1000 km for models 1, 2, and 3, with an incident Rayleigh wave with an azimuth of 30°. Model 1 (open circles) has a crustal thickening of 7 km, model 2 (pluses) has a crustal thickening of 18 km, and model 3 (solid circles) has a crustal thickening of 18 km and a low-velocity layer in the crustal root.

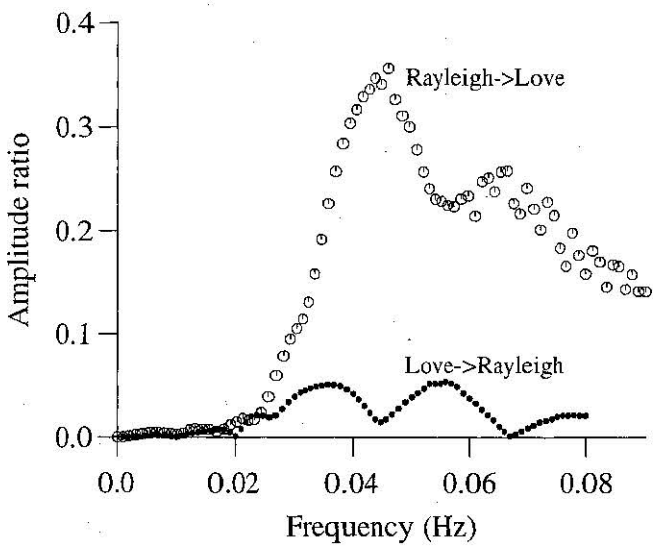

Figure 16. Comparison of Rayleigh to Love and Love to Rayleigh conversion. The curve for Rayleigh to Love conversion (open circles)) is the same as model 2 in Figure 14. The Love to Rayleigh conversion (solid circles) is calculated as the ratio of vertical displacement (at x=2500 km) to transverse displacement (at x=1000 km). In the case of Love to Rayleigh conversion, a fundamental mode Love wave is incident on model 2 with an azimuth of 30°.

with distance due to the interference of different waves. The frequency interval in which wave conversion occurs is approximately the same for the three models. Simulations with intermediate characteristics in terms of crustal thickening and velocities in the crustal root show intermediate Love wave amplitudes.

To show that the observed early wave train can be a Love to Rayleigh converted wave, we also simulated fundamental mode Love waves incident upon a range structure, using the models presented above. These models are not appropriate for the Tornquist Zone. However, they validate whether a range model is also efficient for generating Love to Rayleigh converted waves. Figure 16 compares Rayleigh to Love conversion with Love to Rayleigh conversion, using model 2. In both cases, a surface wave is incident on model 2 with an azimuth of 30°. In the case of Rayleigh to Love conversion, the transverse to vertical amplitude ratio is the same as the one in Figure 16 (model 2). In the case of the Love to Rayleigh conversion, the spectral ratio is calculated between the vertical component at x=2500 km and the transverse component at x=1000 km. The Rayleigh to Love conversion is much stronger than the Love to Rayleigh conversion. In this particular case and distance, the maximum amplitude ratio is approximately 0.05, but at other distances it can be up to 0.1.

The Tornquist Zone is related to a thinning of the crust from east to west and significant changes in the upper mantle [e.g., *Guterch et al.*, 1986; *EUGENO-S Working Group*, 1988; *Zielhuis and Nolet*, 1994]. For the period range considered here, the surface waves are mostly influenced by the crustal structure. We therefore considered a model with a crustal thinning across the Tornquist Zone from 45 km thickness east of it to 35 km west of it, with a linear decrease in crustal thickness over a distance of 20 km. For incident Love waves (with an azimuth of 30°) the Rayleigh wave amplitudes which are created at the crustal thinning vary for several hundred kilometers after which they stabilize as an Airy phase. From this point onwards they have an amplitude of 10% of the amplitude of the incoming Love waves (amplitude ratio of the incoming transverse and the converted vertical). Considering that this somewhat underestimates the converted vertical/transverse ratio (see section 3.2), this seems to fit fairly well with

Table 3. Main parameters of the three models used in the numerical simulations

Model No	Tarim crustal thickness km	Tien Shan crustal thickness km	Low velocity layer
1	42	49	No
2	37	55	No
3	37	55	Yes

the observed amplitude ratio. The Rayleigh wave has a peak spectral amplitude at a period of 22 s, which lies within the frequency range for which the early wave train is observed. The distance dependent amplitude of the converted wave shows why the early wave train is not observed at stations HAM and CLZ as these two stations are the ones located the closest to the Tornquist Zone.

4. Conclusions

Most seismic records from explosions in Lop Nor show anomalously high Love wave amplitudes in the frequency interval between 0.015 and 0.045 Hz. The Love wave spectrum is observed to be rather smooth, while the Rayleigh wave spectrum contains peaks and troughs. Records from explosions in Semipalatinsk do not have such anomalies. This confines the origin of the high Love wave amplitudes to the source or to path effects close to the source.

The numerical simulations show that significant Love wave amplitudes are created by conversion of Rayleigh waves in the Tien Shan model, approximately in the same frequency interval as the Love wave anomalies in the observed data. The Love wave amplitudes are up to 0.35 times the amplitude of the Rayleigh waves that are incident upon the structure. Conversion effects can therefore be expected to be found in observed data.

The simulated Love wave spectrum is smooth, with the maximum amplitude located between 0.04 and 0.05 Hz. The simulated Rayleigh wave spectrum, on the contrary, contains peaks and troughs. This behavior is in qualitative agreement with the observed spectra which show a more complex pattern with peaks and troughs probably due to multiple interference between direct and converted waves.

On the other hand, the simulated Love wave amplitudes are too small to match the observed ones. Even though the simulated transverse/vertical ratios somewhat underestimate what would be observed in real data (see subsection 3.2), the transverse/vertical ratio of up to 10 as observed in the real seismic records are not explained by the simulations. However, this mismatch does not mean that path effects should be discarded. Indeed, our simulations show that variations of crustal thickness are expected to produce strong path effects in the frequency interval 0.02 and 0.1 Hz where anomalous surface waves are observed in this study. In addition, the similarity of anomalies created by explosions with different yield is consistent with path effects. Finally, towards the north, where the structures are comparatively more simple than towards the south, one particular aspect of the observed anomalies can be explained by path effects: the decrease of the transverse/vertical ratio with azimuth (KONO, FLN, and OBN as compared to KEV and WMQ) can then be attributed to the decrease of azimuth of the incoming waves upon the Tien Shan. Yet we do not deny the possible role of tectonic release in generating surface wave anomalies.

The simulation of path effects could be improved in different ways. First, the real Earth structure is three dimensional, while the model we used is two dimensional. Second, anisotropy in the upper mantle and/or lower crust was not considered. Finally, the simulations presented here do not take into account the near field of the seismic source. A knowledge of the precise geometries and elastic properties of the crust and upper mantle are also necessary to improve the modeling of anomalies observed at individual stations.

Our numerical results nevertheless show that converted surface waves can play an important role in surface wave propagation anomalies. This point is confirmed by the Love to Rayleigh converted wave observed in France and Germany. The observation of this wave is possible because of the anomalously high Love wave amplitudes from explosions in Lop Nor. Even with a Love to Rayleigh wave conversion of 5 to 10% amplitude, it is in this particular case sufficient to create a converted wave with approximately the same amplitude as the "ordinary" Rayleigh waves.

Significant wave conversions can obscure the source effects and bias the surface wave tomography of the lithosphere. Note that these findings are particularly significant in the frequency domain used to estimate surface wave magnitude. On the other hand, systematic mapping of such converted waves should make it possible to image lateral changes in the lithosphere using surface waves observed at teleseismic distances.

Acknowledgments. Data from the LDG, GEOSCOPE, and GRSN networks were used, and supplementary data were obtained through the IRIS data management center. Discussions with J.-L. Plantet and Y. Menechal are gratefully acknowledged. We thank P. Benoist and E. Thauvin for drawing the maps. The numerical simulations were carried out at the Centre de Calcul Intensif of the Observatoire de Grenoble, France. We thank the associate editor, A. Levshin, and two anonymous reviewers for constructive comments to the original manuscript.

References

Aki, K., and Y.-B. Tsai, Mechanism of Love-wave excitation by explosive sources, *J. Geophys. Res.*, *77*,, 1452-1475, 1972.

Allen, M. B., B. F. Windley, Z. Chi, and G. Jinghui, Evolution of the Turfan Basin, Chinese central Asia, *Tectonics, 12,* 889-896, 1993.

Archambeau, C. B., and C. Sammis, Seismic radiation from explosions in prestressed media and the measurement of tectonic stress in the Earth, *Rev. Geophys., 8,* 473-499, 1970.

Avouac, J.-P., P. Tapponnier, M. Bai, H. You, and G. Wang, Active faulting and folding in the northern Tien Shan and rotation of Tarim relative to Dzungaria and Kazakhstan, *J. Geophys. Res., 98,* 6755-6804, 1970.

Brandon, C., and B. A. Romanowicz, A no-lid zone in central Chang Tang platform of Tibet: Evidence from pure path phase velocity measurements of long-period Rayleigh waves, *J. Geophys. Res., 91,* 6547-6564, 1986.

Burov, E. V., M. G. Kogan, H. Lyon-Caen, and P. Molnar, Gravity anomalies, the deep structure, and dynamic pro-

cesses beneath the Tien Shan, *Earth Planet. Sci. Lett., 96,* 367-383, 1990.

Capon, J., Analysis of Rayleigh-wave multipath propagation at LASA, *Bull. Seismol. Soc. Am., 60,* 1701-1731, 1970.

Chen, W. P., and P. Molnar, Constraints on the seismic wave velocity structure beneath the Tibetan Plateau and their tectonic implications, *J. Geophys. Res., 86,* 5937-5962, 1981.

Cotton, F., and J.-P. Avouac, Crustal and upper-mantle structure under the Tien Shan from surface-wave dispersion, *Phys. Earth Planet. Inter., 84,* 95-109, 1994.

Dziewonski, A. M., S. Bloch, and M. Landisman, A technique for the analysis of transient seismic signals, *Bull. Seismol. Soc. Am., 59,* 427-444, 1969.

Ekström, G., and P. G. Richards, Empirical measurements of tectonic moment release in nuclear explosions from teleseismic surface waves and body waves, *Geophys. J. Int., 117,* 120-140, 1994.

EUGENO-S Working Group, Crustal structure and tectonic evolution of the transition between the Baltic Sheild and the North German Caledonides (the EUGENO-S Project), *Tectonophysics, 150,* 253-348, 1988.

Gupta, H. K. and H. Narain, Crustal structure of the Himalayan and Tibet Plateau region from surface wave dispersion, *Bull. Seismol. Soc. Am., 57,* 235-248, 1967.

Guterch, A., M. Grad, R. Materzok, and E. Perchuc, Deep structure of the Earth's crust in the contact zone of the Palaeozoic and Precambrian Platforms in Poland (Teisseyre-Tornquist Zone), *Tectonophysics, 128,* 251-279, 1986.

Harkrider, D. G., J. L. Stevens, and C. B. Archambeau. Theoretical Rayleigh and Love waves from an explosion in prestressed source regions, *Bull. Seism. Soc. Am., 84,* 1410-1442, 1994.

Hirn, A., A. Nercessian, M. Sapin, G. Jobert, X. Z. Xin, G. E. Yuan, L. E. Yuan, and T. J. Wen, Lhasa block and bordering sutures: A continuation of a 500-km Moho traverse through Tibet, *Nature, 307,* 25-27, 1984.

Its, E. N., and T. B. Yanovskaya, Propagation of surface waves in a half-space with vertical, inclined or curved interfaces, *Wave Motion, 7,* 79-94, 1985.

Keilis-Borok, V. I. (Ed.), *Seismic Surface Waves in a Laterally Inhomogeneous Earth,* 294 pp., Kluwer Academic Publishers, Norwell, Mass., 1989.

Kosarev, G. L., N. V. Petersen, L. P. Vinnik, and S. W. Roecker, Receiver functions for the Tien Shan analog broadband network: Contrasts in the evolution of structures across the Talasso-Fergana fault, *J. Geophys. Res., 98,* 4437-4448, 1993.

Levshin, A. L., and M. H. Ritzwoller, Characteristics of surface waves generated by events on and near the Chinese nuclear test site, *Geophys. J. Int., 123,* 131-148, 1995.

Ma, X., Lithospheric dynamic map of China and adjacent areas with explanatory notes, scale 1:4,000,000, Geol. Publ. House, Beijing, 1987.

Massé, R. P., Review of seismic source models for underground nuclear explosions, *Bull. Seismol. Soc. Am., 71,* 1249-1268, 1981.

McGarr, A., Amplitude variations of Rayleigh waves: Horizontal refraction, *Bull. Seismol. Soc. Am., 59,* 1307-1334, 1969.

Nolet, G., Partitioned waveform inversion and two-dimensional structure under the Network of Autonomously Recording Seismographs, *J. Geophys. Res., 95,* 8499-8512, 1990.

Pavlis, G. L. H., and H. Mahdi, Surface wave propagation in central Asia: Observations of scattering and multipathing with the Kyrgyzstan broadband array, *J. Geophys. Res., 101,* 8437-8455, 1996.

Pedersen, H. A., M. Campillo, and N. Balling, Changes in the lithospheric structure across the Sorgenfrei-Tornquist Zone inferred from dispersion of Rayleigh waves, *Earth Planet. Sci. Lett., 128,* 37-46, 1994.

Pedersen, H. A., V. Maupin, and M. Campillo, Wave diffraction in multilayered media with the Indirect Boundary Element Method: Application to 3-D diffraction of long-period surface waves by 2-D structures, *Geophys. J. Int., 125,* 545-558, 1996.

Perrier, G., and J. C. Ruegg, Structure profonde du Massif Central Francais, *Ann. Geophys., 29,* 435-502, 1973.

Press, F., and C. B. Archambeau, Release of tectonic strain of underground nuclear explosions, *J. Geophys. Res., 67,* 337-343, 1962.

Roecker, S. W., T. M. Sabitova, L. P. Vinnik, Y. A. Burmakov, M. I. Golvanov, R. Mamatkanova, and L. Munirova, Three-dimensional elastic wave velocity structure of the western and central Tien Shan, *J. Geophys. Res., 98,* 15779-15795, 1993.

Snieder, R., Three-dimensional linearized scattering of surface waves and a formalism for surface wave holography, *Geophys. J. R. Astron. Soc., 84,* 581-605, 1986.

Tanimoto, T., Modelling curved surface wave paths: Membrane surface wave synthetics, *Geophys. J. Int., 102,* 89-100, 1990.

Tapponnier, P., and P. Molnar, Active faulting and Cenozoic tectonics of the Tien Shan, Mongolia, and Baykal regions, *J. Geophys. Res., 84,* 3425-3459, 1979.

Windley, B. F., M. B. Allen, C. Zhang, Z. Y. Zhao and G. R. Wang, Paleozoic accretion and Cenozoic redeformation of the Chinese Tien Shan range, Central Asia, *Geology, 18,* 128-131, 1990.

Wittlinger, G., et al., Seismic tomography of Northern Tibet and Kunlun: Evidence for crustal blocks and mantle velocity contrast, *Earth Planet. Sci. Lett., 139,* 263-279, 1996.

Zhang, J., Polarization characteristics of seismic waves from the May 21, 1992, Lop Nor nuclear explosion using IRIS/GSN broadband data, in *Proceedings of the 16th Annual AFOSR Seismic Research Symposium,* 7-9 Sept. 1994, Thornwood, NY, edited by J. Cipar, J. Lewkowicz, and J. McPhetres, *Rep. PL-TR-94-2217,* Phillips Lab., Hanscom AFB, Mass., 1994.

Zielhuis, A., and G. Nolet, Deep seismic expression of an ancient plate boundary in Europe, *Science, 265,* 79-91, 1994.

J.-P. Avouac, Laboratoire de Détection et de Géophysique, BP 12 92680 Bruyères-le-Châtel, France. (e-mail: avouac@ldg.bruyeres.cea.fr)

M. Campillo and H. A. Pedersen, Laboratoire de Géophysique, Interne et Tectonophysique, Université Joseph Fourier, 38041 Grenoble Cedex, France. (e-mail: Michel.Campillo@obs.ujf-grenoble.fr; Helle.Pedersen@obs.ujf-grenoble.fr)

(Received March 14, 1997; revised December 15, 1997; accepted December 26, 1997.)